

Phase Lags of QPOs in Microquasar GRS 1915+105

Wei Cui

Center for Space Research, Massachusetts Institute of Technology, Cambridge, MA 02139;
 cui@space.mit.edu

ABSTRACT

I report the discovery of hard X-ray phase lags associated with the famous 67 Hz quasi-periodic oscillation (QPO) in microquasar GRS 1915+105. The QPO is seen on multiple occasions. For this investigation, I have chosen one particular observation when the oscillation is the strongest. The measured hard lags show strong energy dependence. With respect to the 2-2.5 keV band, the phase lag increases from insignificant detection at 5.2-7.0 keV to as much as 2.3 radians (which corresponds a time lag of \sim 5.6 ms) above \sim 13 keV. Also detected in the same observation are one narrowly peaked, strong QPO at 67 mHz, along with its first three harmonics, one weak QPO at \sim 400 mHz and one broad QPO at \sim 840 mHz. Similar cross spectral analyses have been performed on these QPOs (and the harmonics), in order to measure any phase lags associated with the features. Phase lags are detected in all, with similar energy dependence. For the 67 mHz QPO, the results are quite intriguing: only the first and third harmonic components show hard lags, while the fundamental and the second harmonic components actually display smaller *soft* lags. Coupled with the energy dependence of the QPO amplitude, the results seem to indicate a complicated change in the signal profile with photon energy. I will discuss the implication of the phase lags on possible origins of the QPOs.

Subject headings: black hole physics – stars: individual (GRS 1915+105) – stars: oscillations – X-rays: stars

1. Introduction

Black hole candidates (BHCs) are known to vary strongly in X-ray (van der Klis 1995; Cui 1999). The variability can sometimes show a characteristic periodicity, in the form of a quasi-periodic oscillation (QPO). For BHCs, QPOs were initially observed only in a few sources at very low frequencies (< 1 Hz), with the exception of the rare “very-high-state” (VHS) QPOs at a few Hz observed of GX 339-4 and GS 1124-68 (van der Klis 1995 and references therein). Since the launch of Rossi X-ray Timing Explorer (RXTE; Bradt et al. 1993), new QPOs have been discovered at an accelerated pace, thanks to the advanced instrumentation of RXTE. Not only are the QPOs now seen in more BHCs, they are also detected at increasingly higher frequencies

(Cui 1999 and references therein). The phenomenon now spans a broad spectrum from a few mHz to several hundred Hz. Despite the observational advances, the origin of QPOs remains uncertain. Progress has been made empirically by correlating the observed properties of the QPOs, such as centroid frequency and amplitude, to physical quantities, such as photon energy and X-ray flux (or mass accretion rate). It has been shown that the correlations can be quite different for different QPOs, perhaps indicating that for BHCs the QPOs form a heterogeneous class of phenomena (Cui 1999; Cui et al. 1999a).

GRS 1915+105 is one of only three known BHCs that occasionally produce relativistic radio jets with superluminal motion (Mirabel & Rodriguez 1999 and references therein). These sources are often referred to as microquasars. First discovered in X-ray (Castro-Tirado et al. 1992), GRS 1915+105 has been studied extensively at this wavelength. Recent RXTE observations revealed a great variety of QPOs associated with the source (Morgan et al. 1997), in addition to its complicated overall temporal (as well as spectral) behaviors (e.g., Greiner et al. 1996). The most famous of all is the QPO at 67 Hz. At the time, it was the highest-frequency QPO ever detected in BHCs. More interestingly, the centroid frequency of the QPOs hardly varies with X-ray flux (Morgan et al. 1997), unlike a great majority of other QPOs. Suggestions have subsequently been made to associate the feature to the dynamical processes in the immediate vicinity of the central black hole, where general relativistic effects may be strongly manifested (Morgan et al. 1997; Nowak et al. 1997; Cui et al. 1998). As a result, a lot of excitement has been generated by the prospect of using such signals to test the general theory of relativity in the strong-field limit (Cui et al. 1999b and references therein). Before this ultimate goal can be reached, however, it is clearly important to best characterize and understand this particular QPO observationally. In this Letter, I report the discovery of an important property of the feature: the oscillation lags more behind at higher photon energies. Some of the results have already been presented elsewhere in preliminary form (Cui 1997; Cui 1999).

2. Observations

The 67 Hz QPO has been detected in various different states of GRS 1915+105 (Morgan et al. 1997). For this investigation, I have selected one RXTE observation when the oscillation appears the strongest (based on Morgan et al. 1997). The observation was made on May 5, 1996, when the source was in a bright state, with a total exposure time about 10 ks. Multiple high-resolution timing modes were adopted for the observation. Considering the trade-off between statistics and energy resolution, I have decided to rebin the $16\mu s$ *Event* data to 2 ms and to combine the sixteen energy bands (above ~ 13 keV) into one. I have then merged the *Event* mode data with the 2 ms *Binned* mode data (which covers four energy bands below ~ 13 keV). Now, a total of 5 energy bands are available for carrying out subsequent analyses. The bands are approximately defined as 2–5.2 keV, 5.2–7.0 keV, 7.0–9.6 keV, 9.6–13.2 keV, and 13.2–60 keV.

3. Data Analysis and Results

A collection of power-density spectra (PDS) of GRS 1915+105 can be found in Morgan et al. (1997), for the initial 31 RXTE observations of the source, but only in one energy band (2–20 keV). Of great interest here is the energy dependence of the temporal properties of the source, so I have constructed the PDS (with the deadtime-corrected Poisson noise power subtracted) in the five energy bands defined. Fig. 1 shows the results. The presence of QPOs is apparent. Most prominent is the one centered at about 67 mHz, along with its first three harmonics. As noted by Morgan et al. (1997), the amplitude of the fundamental component seems to follow a general decreasing trend toward high energies, while that of the harmonics shows just the opposite. The 67 Hz QPO is clearly visible in the PDS, especially at high energies. Also detected are a weak QPO at about 400 mHz (which is missing from Morgan et al. 1997) and a broad QPO at about 840 mHz.

To be more quantitative, I have fitted the PDS with an empirical model consisting of Lorentzian functions for the QPOs and a double-broken power law for the underlying continuum. I have limited the frequency range to roughly 0.001–10 Hz during the fitting to focus on the low-frequency QPOs, since the 67 Hz QPO has already been quantified (Morgan et al. 1997). Table 1 summarizes the best-fit centroid frequency and width for each QPO at low frequencies, derived from the 7.0–9.6 keV band (which is chosen as a compromise between the signal strength and the data quality). Fig. 2 shows the fraction rms amplitude of each QPO at different energies. The 400 mHz QPO and the 840 mHz QPO, as well as the 67 Hz QPO (Morgan et al. 1997), strengthen toward high energies (with a hint of saturation), similar to most QPOs of BHs (Cui 1999). The behavior of the 67 mHz QPO is, however, more complicated and very intriguing: while the harmonics of the QPO follow the usual trend, the fundamental component becomes stronger first and then weakens significantly at higher energies, with the amplitude peaking at 8–9 keV.

To derive phase lags, I have chosen the 2–5.2 keV band as a reference band, and computed a cross-power spectrum (CPS) between it and each of the higher energy bands. Note that the final CPS represents an ensemble average over the results from multiple 512-second segments of the time series (similarly for the PDS shown). The phase of the CPS represents a phase shift of the light curve in a selected energy band with respect to that of the reference band. Here, I follow the convention that a positive phase indicates hard X-rays lagging behind soft X-rays, i.e., a hard lag. The uncertainty of the phase is estimated from the standard deviation of the real and imaginary parts of the CPS. The magnitude of the QPO lags is derived from fitting the profile of the lags with Lorentzian functions at the QPO frequencies which are fixed during the fitting. Note that for the 67 Hz QPO I have also fixed the width of the profile to that of the QPO (see Table 2 in Morgan et al. 1997), due to the lack of statistics. The measured lags are plotted in figures 3 and 4 for the 67 Hz QPO and other low-frequency QPOs, respectively. The errors are derived by varying the parameters until $\Delta\chi^2 = 1$ (i.e., corresponding roughly to 1σ confidence intervals; Lampton et al. 1976).

Most QPOs show significant hard lags. Surprisingly, however, the odd harmonics of the 67 mHz QPO display *soft* lags. It is clear that the QPO lags depend strongly on photon energy — the higher the energy the larger the lag, with the exception of the 840 mHz QPO where the measured hard lag increases first and then drops above 13 keV. For the 67 Hz QPO, the phase lag reaches as high as 2.3 radians, which is equivalent to a time lag of about 5.6 ms. The phase lags are smaller for low-frequency QPOs, but the corresponding time lags are quite large. For instance, the first harmonic of the 67 mHz QPO shows a time lag greater than 1 second for the highest energy band.

4. Discussion

It is known that hard lags are associated with the X-ray emission from BHCs (van der Klis 1995; Cui 1999). Although the studies of hard lags are mostly based on broad-band variability, the large lags associated with the VHS QPOs of GS 1124-68 have been noted (van der Klis 1995).

Often, the hard lags are attributed to thermal inverse-Comptonization processes (e.g., Miyamoto et al. 1988; Hua & Titarchuk 1996; Kazanas et al. 1997; Böttcher & Liang 1998; Hua et al. 1999), which are generally thought to be responsible for producing the hard power-law tail of X-ray spectra of BHCs (Tanaka & Lewin 1995). In these models, the lags are expected to be larger for photons with higher energies, since a greater number of scatterings are required for seed photons to gain enough energy. More quantitatively, the hard lags, which indicate the diffusion timescales through the Comptonizing region, should scale logarithmically with photon energy (e.g., Payne 1980; Hua & Titarchuk 1996); this roughly agrees with the observations (Cui et al. 1997; Crary et al. 1998; Nowak et al. 1999; also see figures 3 and 4). However, the measured time lags can often be quite large, e.g., a few tenths of a second, at low frequencies, which would require a large hot electron corona (roughly one light second across; Kazanas et al. 1997; Böttcher & Liang 1998; Hua et al. 1999). A even larger corona would be needed to account for the hard lags observed of the first harmonic of the 67 mHz QPO in GRS 1915+105. It is still much debated whether the required corona can be maintained physically (Nowak et al. 1999; Böttcher & Liang 1998; Poutanen & Fabian 1999). Also, the observed soft lags of the 67 mHz QPO (and its second harmonic) are entirely incompatible with the Compton models. On the other hand, the smaller time lags associated with the QPOs at higher frequencies (e.g., the 67 Hz QPO) can still be accommodated by the models. Like the QPOs themselves, the phase lags may very well be of multiple origins.

Another class of models link the time lags to the propagation or drift time scales of waves or blobs of matter through an increasingly hotter region, toward the central black hole, where hard X-rays are emitted (Miyamoto et al. 1988; Böttcher & Liang 1998). In this scenario, as the disturbance (such as waves, blobs, and so on) propagates, its X-ray spectrum hardens, producing the observed hard lags. The models can also produce the logarithmic energy dependence of the hard lags (Böttcher & Liang 1998). The origin of clumps of matter may lie in the Lightman-Eardley instability which sets in wherever radiation pressure dominates over gas pressure in the accretion

disk (Lightman & Eardley 1974). It has recently been proposed that such a condition is perhaps generally met for the inner region of accretion disks in BHCs and thus the presence of blobs may not be surprising (Krolik 1998). However, it is not clear how to associate QPOs with the dynamics of the blobs. While the Keplerian motion of the blobs could manifest itself in a QPO observationally, any radial drift of the blobs would cause the QPO frequency to increase with energy, which is not observed.

On the other hand, it is perhaps easier to associate QPOs with traveling waves. For instance, Kato (1989) suggested that the propagation of corrugation-mode oscillations might explain the hard lags observed of BHCs. Note also that inward-propagating perturbations have recently been invoked to explain the X-ray variability of BHCs (Manmoto et al. 1996), in the context of advection-dominated accretion flows (ADAFs; e.g., Narayan & Yi 1994). In general, recent works seem to converge toward an ADAF-like geometry for the accretion flows around black holes, i.e., an inner quasi-spherical, optically thin region and an outer thin, optically thick disk (e.g., Narayan & Yi 1994; Chen et al. 1995; Dove et al. 1997; Luo & Liang 1998). Applied to GRS 1915+105, the wave-propagation models might be able to account for the hard lags observed of the QPOs, although the required speed of propagation would be quite small (much smaller than that of free fall) in some cases. Moreover, the peculiar behavior of the 67 mHz QPO — the even harmonics showing soft lags while the odd harmonics hard lags — can perhaps be explained by invoking a significant change in the wave form as the wave propagates. To better illustrate this point, I have simulated an oscillation of fundamental frequency 67 mHz that also includes the first three of its harmonics. A sine function is used to describe each harmonic component, which uses the measured fractional rms amplitude and phase of each component of the 67 mHz QPO in GRS 1915+105. The overall profiles of the simulated oscillation are constructed by summing up the four components for the 2–2.5 keV band (the reference band in which the phases are initialized to zero) and the 13.2–60 keV band, respectively. They are shown in Fig. 5. The inferred evolution of the oscillation profile is quite drastic. The soft and hard lags are mixed together in the figure, contributing to the overall variation of the wave form. But, because the hard lag is so dominating, it can be still be recognized by comparing the times of the minimum points between the two profiles. However, the models cannot naturally explain why the fractional amplitude of the QPOs increases with energy if the QPOs are of disk origin (Cui 1999); neither can most Compton models, unless a certain spatial distribution of the Compton y -parameter is assumed (Wagoner et al. 1999; Lehr et al. 1999).

A third class of models associate the hard lags with dynamical processes in Comptonizing regions themselves. Poutanen & Fabian (1999) proposed that the time lags may be identified with the spectral hardening of magnetic flares as the magnetic loops inflate, detach and move away from the accretion disk. Now, the time lags are directly related to the evolution timescales of the flares. This model differs fundamentally from others in allowing Comptonizing regions to vary. It, therefore, provides an interesting possibility that the QPOs of BHCs might be an observational manifestation of the oscillatory nature of these regions. The oscillation may occur, for example,

in the temperature of hot electrons and/or in the Compton optical depth, both of which cause “pivoting” of the Comptonized spectrum. The spectral pivoting might naturally explain the observed energy dependence of the QPO amplitude (e.g., Lee & Miller 1998; see Kazanas & Hua 1999 for another possibility).

To summarize, besides other observable properties of the QPOs, the phase lags provide additional information that may be critical for our understanding of the QPO origins. The energy dependence of the lags has already had serious implications on theoretical models — Comptonization seems always required. It might also shed light on the evolution of intrinsic wave forms, when combined with the energy dependence of the QPO amplitude, and thus on underlying physical processes and conditions that can cause the evolution. Moreover, the magnitude of the lags might provide a direct measure of such important physical properties of the system as the size of the Comptonizing region, or the propagation speed of disturbances in accretion flows, or the evolution timescales of magnetic flares originating in the accretion disk. Therefore, the QPO lags might ultimately prove essential for understanding the geometry and dynamics of mass accretion processes in BHCs.

I gratefully acknowledge useful discussions with many participants of the first Microquasar Workshop (which was held in May, 1997 at the Goddard Space Flight Center, Greenbelt Maryland) where some of the preliminary results were first presented. I thank the referee, Dr. Bob Wagoner, for his prompt report and many useful comments. Financial support for this work is partially provided by NASA through an LTSA grant and several RXTE grants.

REFERENCES

Böttcher, M., & Liang, E. P. 1998, *ApJ*, 506, 281

Böttcher, M., & Liang, E. P. 1999, *ApJ*, 511, L37

Bradt, H. V., Rothschild, R. E., & Swank, J. H. 1993, *A&AS*, 97, 355

Castro-Tirado, A. J., Brandt, S., & Lund, N. 1992, *IAU Circ.* 5590

Chen, X., et al. 1995, *ApJ*, 443, L61

Crary, D. J., et al. 1998, *ApJ*, 493, 71

Cui, W., Zhang, S. N., Focke, W., & Swank, J. H. 1997, *ApJ*, 484, 383

Cui, W. 1997, talk at the Microquasar Workshop, Goddard Space Flight Center, Greenbelt, Maryland, May 1-3

Cui, W., Zhang, S. N., & Chen, W. 1998, *ApJ*, 492, L53

Cui, W. 1999, Proc. “High-Energy Processes in Accreting Black Holes”, eds. J. Poutanen & R. Svensson (ASP: San Francisco), *ASP Conf. Ser.* Vol. 161, P. 97 (astro-ph/9809408)

Cui, W., Zhang, S. N., Chen, W., & Swank, J. 1999a, talk at the 193rd American Astronomical Society Meeting, *BAAS*, vol. 30, No. 4

Cui, W., Chen, W., & Zhang, S. N. 1999b, Proc. “The Third William Fairbank Meeting on The Lense-Thirring Effect”, eds. L.-Z. Fang & R. Ruffini, in press (astro-ph/9811023)

Dove, J. B., Wilms, J., Maisack, M., & Begelman, M. C. 1997, *ApJ*, 487, 759

Greiner, J., Morgan, E. H., & Remillard, R. A. 1996, *ApJ*, 473, L107

Hua, X.-M., & Titarchuk, L. 1996, *ApJ*, 496, 280

Hua, X.-M., Kazanas, D., & Cui, W. 1999, *ApJ*, 512, 793

Kato, S. 1989, *PASJ*, 41, 745

Kazanas, D., Hua, X.-M., & Titarchuk, L. 1997, *ApJ*, 480, 735

Kazanas, D., & Hua, X.-M. 1999, *ApJ*, 519, 750

Krolik, J. H., *ApJ*, 498, L13

Lampton, M., Margon, B., & Bowyer, S. 1976, *ApJ*, 208, 177

Lee, H. C., & Miller, G. S. 1998, *MNRAS*, 299, 479

Lehr, D. E., Wagoner, R. V., & Wilms, J. 1999, *BAAS*, 31, 731

Lightman, A. P., & Eardley, D. M. 1974, *ApJ*, 187, L1

Luo, C., & Liang, E. P. 1998, *ApJ*, 498, 307

Manmoto, T., Takeuchi, M., Mineshige, S., Matsumoto, R., & Negoro, H. 1996, *ApJ*, 464, L135

Mirabel, I. F., & Rodriguez, L. F. 1999, *ARA&A*, vol. 37, in press (astro-ph/9902062)

Miyamoto, S., Kitamoto, S., Mitsuda, K., & Dotani, T. 1988, *Nature*, 336, 450

Morgan, E. M., Remillard, R. A., & Greiner, J. 1997, *ApJ*, 482, 993

Narayan, R., & Yi, I. 1994, *ApJ*, 428, L13

Nowak, M. A., Wagoner, R. V., Begelman, M. C., & Lehr, D. E. 1997, *ApJ*, 477, L91

Nowak, M. A., Vaughan, B. A., Wilms, J., Dove, J. B., & Begelman, M. C. 1999, *ApJ*, 510, 874

Payne, D. G. 1980, *ApJ*, 441, 770

Poutanen, J., & Fabian, A. C. 1999, *MNRAS*, 306, L31

Tanaka, Y., & Lewin, W. H. G. 1995, in “X-ray Binaries”, eds. W. H. G. Lewin, J. van Paradijs, & E. P. J. van den Heuvel (Cambridge U. Press, Cambridge) p. 126

van der Klis, M. 1995, in “X-ray Binaries”, eds. W. H. G. Lewin, J. van Paradijs, & E. P. J. van den Heuvel (Cambridge U. Press, Cambridge) p. 252

Wagoner, R. V., Silbergleit, A. S., Lehr, D. E., & Ortega, M. A. 1999, *BAAS*, 31, 708

Table 1. Low-frequency QPOs in GRS 1915+105

Frequency (mHz)	FWHM (mHz)	Comments
$66.8^{+0.1}_{-0.1}$	$1.2^{+0.2}_{-0.2}$	fundamental component
$133.3^{+0.2}_{-0.2}$	$2.4^{+0.4}_{-0.4}$	first harmonic
$201.2^{+0.3}_{-0.6}$	$4.0^{+0.9}_{-1.0}$	second harmonic
$267.7^{+0.6}_{-0.7}$	$7.4^{+1.1}_{-1.0}$	third harmonic
403^{+2}_{-2}	14^{+8}_{-6}	...
841^{+5}_{-5}	535^{+19}_{-18}	...

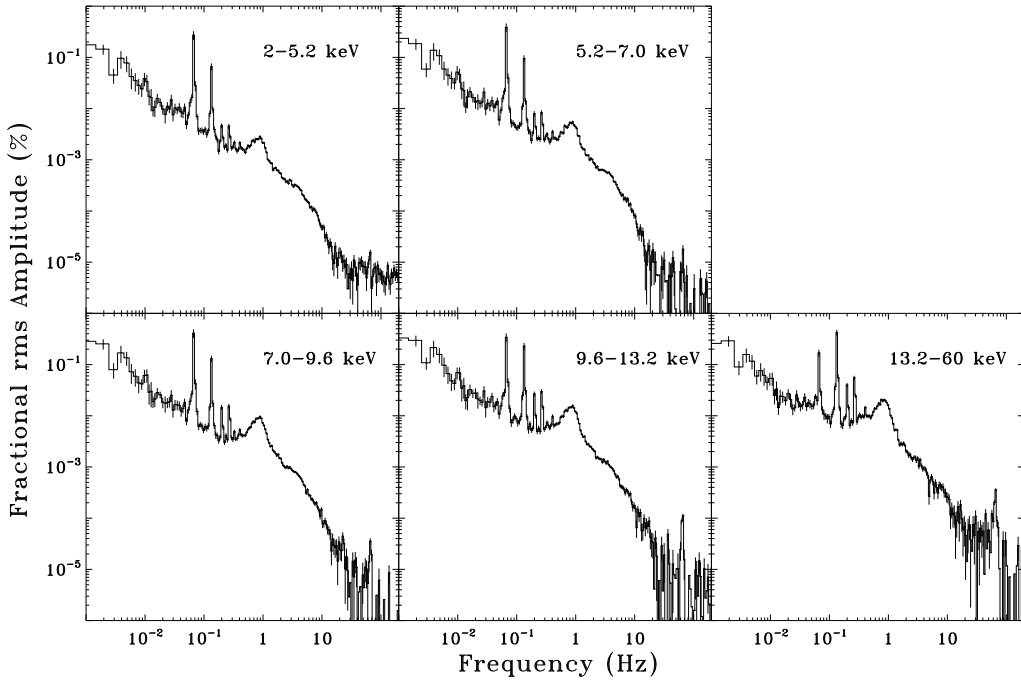


Fig. 1.— Power density spectra of GRS 1915+105 in five energy bands. Note that the dead-time corrected noise power due to counting statistics has been subtracted.

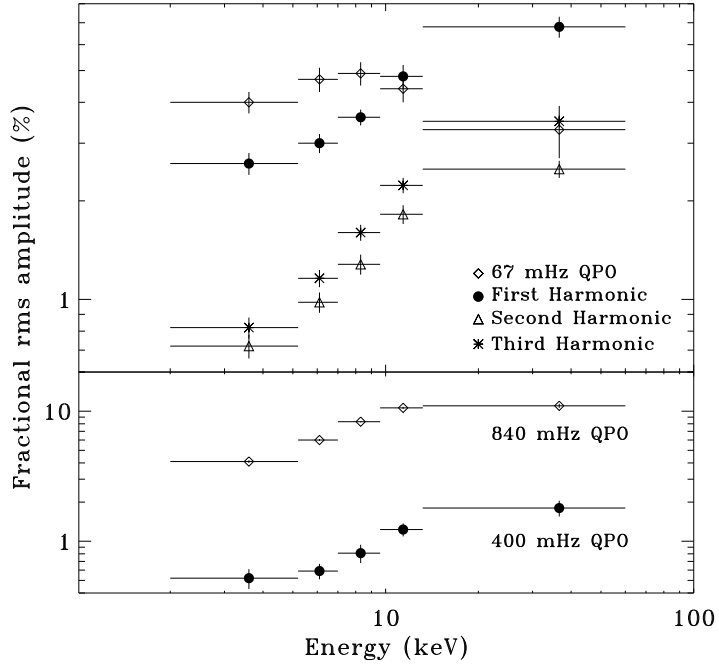


Fig. 2.— Energy dependence of QPO amplitude. Note that the 67 Hz QPO is not shown here; the results can be found in Morgan et al. (1997).

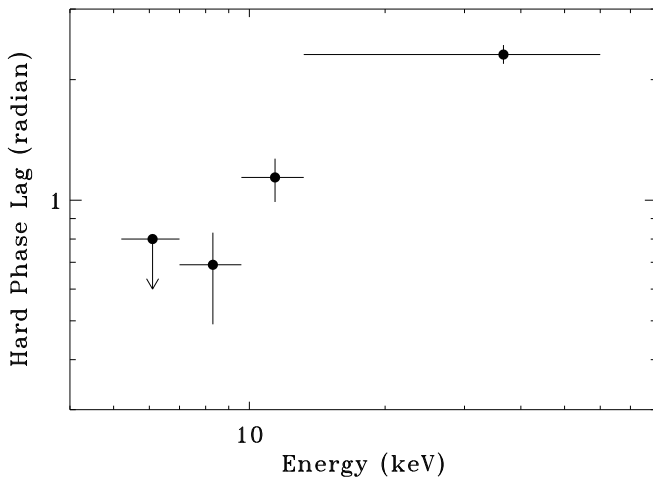


Fig. 3.— Energy dependence of hard phase lag associated with the 67 Hz QPO. The hard lag is not significantly detected in the lowest energy band, so a 3σ upper limit is shown.

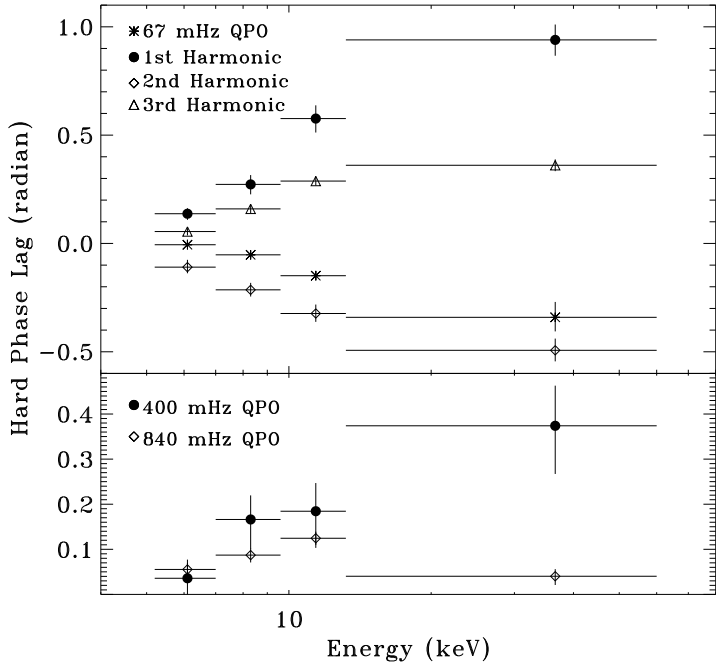


Fig. 4.— Similar to Fig. 3, but for phase lags associated with the low-frequency QPOs. Note that the negative values indicate soft lags.

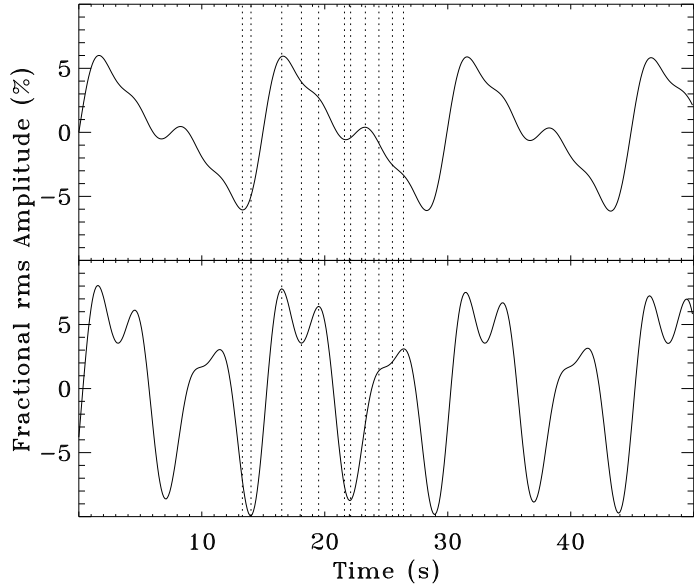


Fig. 5.— Simulated 67 mHz *periodic* signals with three harmonics included. The simulation uses the actual fractional rms amplitude and phase lag of each harmonic component of the 67 mHz QPO in two energy bands, 2–5.2 keV (top panel) and 13.2–60 keV (bottom panel). The dotted line marked all the transition points in each profile for comparison.